Source estimation of an unexpected release of Ruthenium-106 in 2017 using an inverse modelling approach

Luke M. Western[a], Sarah C. Millington[b], Anastasia Benfield-Dexter[a] and Claire S. Witham[b]

[a]School of Chemistry, University of Bristol, UK
[b]Met Office, Exeter, UK

ARTICLE INFO

Keywords:
nuclear incidents, radiological releases, inverse modelling

ABSTRACT

For the first time since the Chernobyl accident, detectable concentrations of ruthenium-106 were measured across Europe in September and October 2017. The source of this radioactive cloud remains unconfirmed. In this paper we present a forensic inverse modelling study to simultaneously estimate the source location, timing and magnitude of the unexpected ruthenium-106 release using 473 measurements of atmospheric concentration. To do this, we introduce a novel method, which estimates the uncertainty in the often unknown transport error using a Markov chain Monte Carlo approach. We corroborate the conclusions of other studies which suggest the source location is in the Southern Ural region of Russia, where the Mayak nuclear complex is located. Assuming that the Mayak nuclear complex is the most plausible release location, the method estimates that 441 $\pm$ 13 TBq was released 12:00-18:00 UTC 24 September 2017, assuming a six hour release window.

1. Introduction

Accidental releases of radiological species range from catastrophic events such as the incident at Chernobyl or Fukushima Daiichi Nuclear Power Plant to small scale releases that are often unnoticed or unreported. Recent years have seen a number of releases that are small as to not pose any immediate danger to the public, but large enough that their atmospheric concentration can be recorded and source attribution is necessary (e.g. Tichý et al., 2017; Masson et al., 2018). From late September 2017 there were detectable concentrations of ruthenium-106 (^{106}Ru) in many European countries for the first time since the Chernobyl accident (Jakab et al., 2018; Penev et al., 2018; Ramebäck et al., 2018; Masson et al., 2019). A small number of sites also detected levels of the isotope ruthenium-103 (e.g. Ramebäck et al., 2018). The source of the release was unknown and remains unconfirmed. A number of emissions sources have been ruled out, such as melting of a radiotherapy source and satellite reentry (Masson et al., 2019). There have been suggestions that the source is the Mayak nuclear complex in Russia, possibly during the production of a high-specific activity ^{144}Ce source (Cartlidge, 2018; Masson et al., 2019), or a release from a ruthenium jet engine (Mietelski and Povinec, 2020).

This paper aims to better understand this 2017 ruthenium release by applying a new method for identifying the source location, magnitude and release time of an unknown release of a radiological species using measurements of atmospheric concentration and an inverse modelling approach. There are a number of inverse methods proposed in the literature for assessing the source term of both unknown (e.g. Delle Monache et al., 2008; Cervone and Franzese, 2010; Annunzio et al., 2012; Tichý et al., 2017; Maffezzoli et al., 2019) and known release locations (e.g. Stohl et al., 2012; Saunier et al., 2013; Liu et al., 2017), and many more to quantify non-radiological atmospheric species (e.g, Michalak et al., 2005; Brunner et al., 2012; Ganesan et al., 2014; Western et al., 2020). The method proposed here aims to be suitable for time-scales for operational response, which needs a well-informed, yet rapid response to a radiological incident with an unknown source. Large scale incidents from known source location may benefit from more computationally intensive inverse algorithms available in the literature (e.g. Yee et al., 2008; Liu et al., 2017; Lucas et al., 2017).

This paper first outlines the measurements and dispersion model set-up used, followed by a description of the inverse method. The results and discussion follows, which proposes the likely release location, time and source magnitude. Finally, we make our concluding remarks.

2. Method

This section details the measurements used to inform the inverse modelling procedure as well as the atmospheric transport model which provides a mapping between the source estimation and measurements.

2.1. Measurements of airborne concentration

Masson et al. (2019) provide a summary of ^{106}Ru measurements of wet and dry deposition and airborne concentrations, as well as a small number of measurements of airborne concentrations of ^{103}Ru. In this paper we limit ourselves to using airborne measurements of ^{106}Ru concentrations (in mBq m^{-3}), as summarised in the Masson et al. (2019) supporting information. This dataset contains 1,069 airborne concentration measurements in 35 countries, with sampling periods lasting from a few hours to several months (please see Masson et al. (2019) and references therein for more information on the sampling techniques for these measurements). Measurements with shorter measurement periods will generally provide more information than those with

ORCID(s):

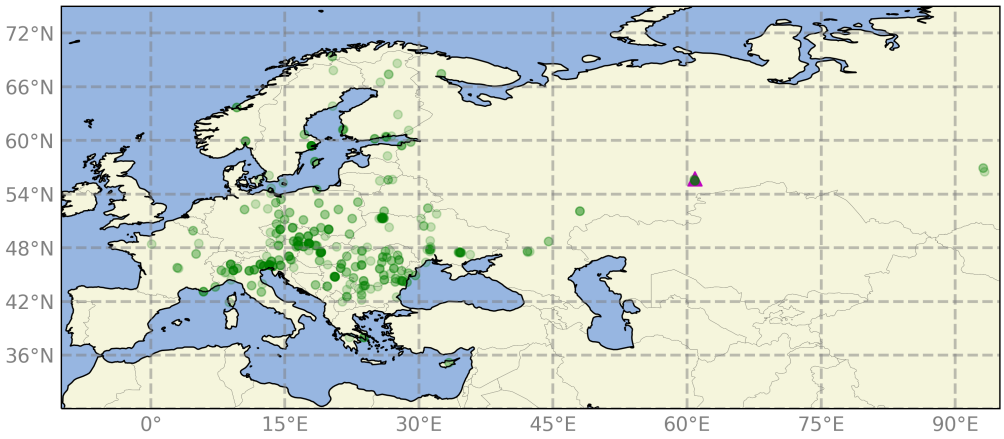

Figure 1: The green semi-transparent circles show the locations of measurements used to estimate the source of ruthenium-106. More opaque circles indicates that more measurements were made at the measurement site. The magenta triangle shows the location of the Mayak nuclear facility.

longer sampling periods, providing that there is sufficient signal-to-noise in the measurements. The air histories for very long measurements periods will be dispersed over large regions, and therefore have lower sensitivities to possible release locations. Many of these measurements are below the detection limit of the instrument, which we exclude from our dataset here. Additionally, we exclude, for computational convenience, three measurements made in Russia where the sampling period was longer than three months. This leaves a total of 473 measurements of ^{106}Ru atmospheric concentration ranging from 1.7×10^{-4} to 176.09 mBq m^{-3}. Figure 1 shows the locations of these measurements. Many, but not all, of these measurements are presented with their associated error, which is given as a two standard deviation error. Where no measurement error is available, we assume that the error is equal to the mean percentage error for all available measurement errors. We use these measurements, and their associated errors, to inform the source estimation.

2.2. Atmospheric transport model

The approach taken here to estimate the source of a radiological release from measurements requires simulating the transport of air sampled by the measurement instrument backwards in time. As the model is backwards running using a radioactive tracer, no deposition processes are considered. The simulation of air history of the measured air sample requires an atmospheric transport model. Here we use the Numerical Atmospheric-dispersion Modelling Environment (NAME, Jones et al., 2007) developed by the UK Met Office. NAME is a Lagrangian transport model, originally created to model the dispersion of radionuclides from incidents such as the Chernobyl incident, and was originally called the Nuclear Accident Model. In this work we choose meteorology from the Met Office Unified Model to drive NAME (Walters et al., 2014).

We simulate the transport from each measurement site in a domain covering the globe with meteorology at 0.140625 by 0.09375°(approximately 10 km over the United Kingdom). The NAME output is produced at a spatial resolution of 0.5 by 0.5°in order to reduce the computation of the inverse method. Each measurement site releases 25,000 particles per hour from the end of the measurement period until its start (see Masson et al. (2019) for the measurement period of each site). Due to the lack of information about the positioning of the measurement sites beyond their cardinal locations, we release the particles in NAME at 20 $\pm$ 10 magl. From the time of release, NAME outputs the time-integrated concentration of a unit mass release rate of a tracer species, which has a half-life of ^{106}Ru of 373.59 days, every six hours on the global grid. The transport is simulated backwards until 06:00 UTC on 20 September 2017. We choose to output the dosage in the bottom 250 metres above ground level (magl) of the domain to define the sensitivity of the measurement to the source. This makes the approach only suitable for near-surface releases and so would be unable to characterise, for example, a radiological release during satellite reentry. The measured ^{106}Ru appears to be mainly in particulate form (Masson et al., 2019), although in the absence of more information of the size distribution and density of these particulates (and the likely paucity of information during future unexpected releases) we found it satisfactory to model the transport of ^{106}Ru as a tracer gas.

We convert the integrated dosage output from NAME into a sensitivity following the approach in Manning et al. (2011). This means that the units of the sensitivity multiplied by the units of the source emissions will equal the mea-

surement units. The difference here is that rather than creating a sensitivity of each measurement to an integrated emission over the entire air history, we instead create a sensitivity to each six hourly period of the air history. This makes the assumption that the release was constant and uniform only over each six hour period. We make the assumption that non-reported accidents are generally from nonreactor facilities, and that the release is limited to a single six hour release period (Elder et al., 1986).

Once the transport has been simulated and the sensitivities have been produced, these can be used within a statistical model to estimate the release source. The resultant sensitivities for all measurement site can be seen as an animation in the supplementary information.

2.3. Inverse methodology

Here we introduce the algorithm for inferring source information about a small radiological release. We apply this method to the case of the 2017 release of Ru-106. We assume throughout that the release is constant over a short release period, for example a short venting or leakage, rather than a sustained release that occurs during catastrophic incidents. The method is for estimating the location, time and magnitude of an unknown release of a known radiological species. This method must be fast so that the estimation process can be carried out operationally, informing the authorities where necessary action must be taken.

The aim of this method is to infer the emission magnitude, x, and time period, t, of a release of a radioactive species at an unknown location given a set of n measurements of airborne concentration contained in the vector $\mathbf{y}$. At a given release time t in a discrete set of possible release times $\mathscr{T}$ we assume the linear model

$$\mathbf{y} = \mathbf{h}(t)x + \epsilon, \tag{1}$$

where $\mathbf{h}(t)$ is a linear mapping from the measurements to the emission, created using the approach in section 2.2 and ϵ is a stochastic error representing the combined error in the simulated transport, which is unknown, and measurements, which we treat as known.

The approach taken here involves estimating the release from all possible locations in a given spatial domain, where each possible release location is a point source within a 0.5°by 0.5°spatial bin in a global domain. This requires inference to be carried out a large number of times. Taking this approach means, however, that inference at each location can be run independently, taking advantage of parallel and high performance computing capabilities. Therefore, we take a hierarchical Bayesian approach to estimate the emission and model-transport error, and take an empirical Bayes approach to estimate the most likely release time $\hat{t}$. There is very little prior information during events of unexpected radiological releases. We therefore use a non-informative Normal prior for x to inform the Bayesian inference, or the Jeffreys prior for x (see e.g. Robert et al., 2009). This does allow x to take any real number value, including negative emissions (unlike e.g. Liu et al., 2017; Tichý et al., 2017), although this assumption remains suitable in practice. We treat the standard deviation of the simulated transport error as unknown, and assume it is identical and independently distributed for all simulations. We estimate this standard deviation during inference and assign a uniform prior which we give bounds of 5 to 50 mBq m^{-3}. By taking an empirical Bayes approach to estimate the release time we rely on maximising the likelihood, or assume that the prior probability is a delta function informed by the data in a Bayesian setting, for example as used in Liu et al. (2017).

To infer the parameters describing the emissions and transport error we use a Markov chain Monte Carlo (MCMC) method, while using Expectation-Maximisation to infer the time of the release. The algorithm is presented in more detail in Appendix A. We build this MCMC approach using three sampling steps at each iteration. The samplers have been chosen for their efficiency and ease of use in a rapid response scenario. The magnitude of the emissions source is sampled using a Gibbs step (Geman and Geman, 1984), followed by a Slice sampling step for the transport error (Neal, 2003) and then an Expectation-Maximisation step for the release time (Dempster et al., 1977). After sampling the variables we extract the mean and standard deviation of the posterior distribution of the sampled x values as the reported estimate of the source emission and its marginalised expectation-maximised time period as the most likely release time. We judge the likely release location on the log-likelihood of the mean posterior of source emissions given the measurements and their errors and mean posterior estimates of the transport error and model release time. This produces a qualitative estimate of the likely source location, where further investigation into the approximate release location may allude to the true emissions source. These inferred estimates allow conclusions to be drawn about the nature of the September 2017 release of ^{106}Ru.

3. Results and discussion

The results in Figure 2(a) show a high likelihood that the release source was in the Southern Ural region of Russia, an area that includes the location of the Mayak nuclear processing facility. This aligns with findings from other modelling studies (Sørensen, 2018; Maffezzoli et al., 2019; Masson et al., 2019; Saunier et al., 2019; Shershakov et al., 2019). The location of the Mayak facility itself does not have the highest likelihood of being the source but, given the region of high likelihood, we are unable to find a different corroborating source. If the Mayak nuclear facility is the assumed source, figure 2(b) shows the most likely release date is 24 September 2017, and a release time, which is not displayed on the figure, of 12:00-18:00 UTC, assuming a six hour release period. Figures 2(c) and 2(d) show the estimated release size of the ^{106}Ru release in each 0.5°by 0.5°spatial bin and its respective one standard deviation uncertainty. At the Mayak nuclear facility, this corresponds to a total release of 441 ± 13 TBq, or 3.6 ± 0.1 g of ^{106}Ru.

Figure 3 shows the simulated transport of ^{106}Ru in the bottom 250 m of the atmosphere by running the NAME

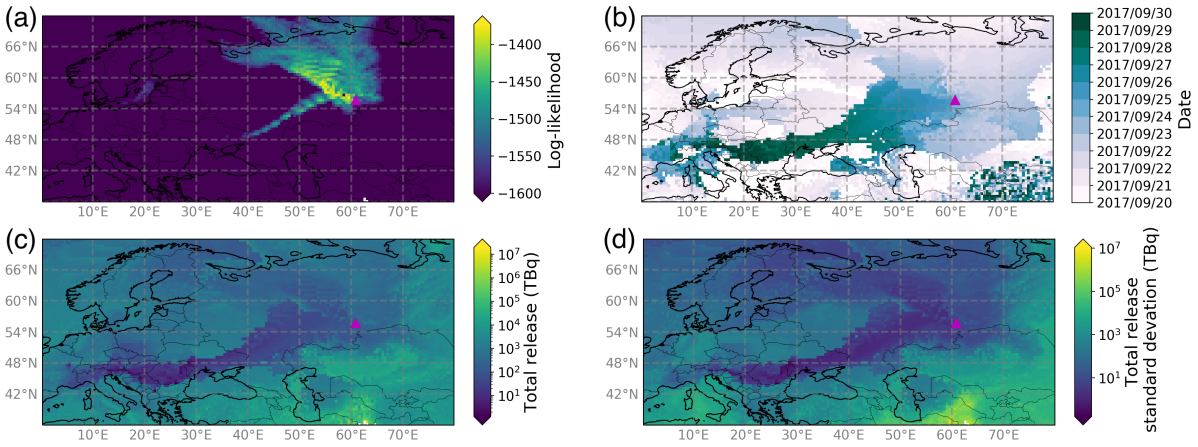

Figure 2: Maps of (a) the estimated location, and, given each location, (b) the estimated date, (c) emission size and (d) uncertainty in the emissions size of the source of an unexpected release of ^{106}Ru in Autumn 2017. The magenta triangle shows the location of the Mayak nuclear facility.

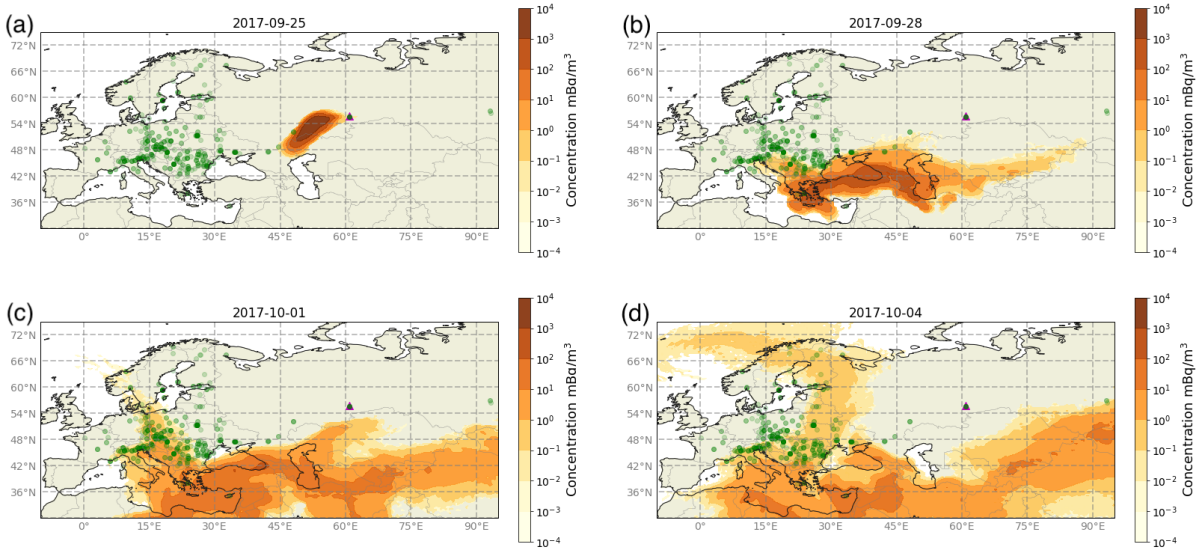

Figure 3: A simulation of the transport of ^{106}Ru from the Mayak nuclear facility with a release of 441 TBq during the period 12:00-18:00 UTC 24 September 2017. The figures show the daily-averaged concentrations in the lowest 250 m of the atmosphere on (a) 25 September, (b) 28 September, (c) 1 October and (d) 4 October 2017. The magenta triangle shows the Mayak nuclear facility and the green circles show the locations of the measurement sites used for the inversion.

model in the forward direction using the source as the Mayak nucelar facility with a release of 441 TBq at a height of 50 ± 50 m released uniformly between 12:00-18:00 UTC 24 September 2017. The modelled airborne concentration at a selection of measurement sites from the forward simulations can be seen in the Figure 4, and generally show good agreement. Figure 5 shows a comparison of the measured ^{106}Ru concentrations and the respective modelled (posterior mean) concentrations for all meaurement sites, assuming a release from the Mayak nuclear facility using the inferred source characteristics using the method in section 2.3. Figure 6 shows the same data for the measured and modelled (posterior mean) concentrations on a scatter plot.

The results found here estimate that the unexpected release of ^{106}Ru in 2017 originated from the Mayak nuclear facility on 24 September 2017 between 12:00-18:00 UTC and released 441 TBq of ^{106}Ru into the atmosphere. Our estimate of 12:00-18:00 UTC 24 September 2017 is earlier than the estimated release date by Masson et al. (2019) at between 18:00 UTC 25 September 2017 and 12:00 UTC 26 September 2017 and and the estimate by Sørensen (2018) of a 05:00-13:00 UTC 26 September 2017 release, but falls closer in line with the earlier estimated release date made by Shershakov et al. (2019). Saunier et al. (2019) estimate a time series release, with a smaller release (< 2 TBq) on 23 and 24 September 2017, and a larger release (∼ 250 TBq) on 26 September. The total estimated release is 252 ± 13 TBq, which is significantly smaller than the release estimated in

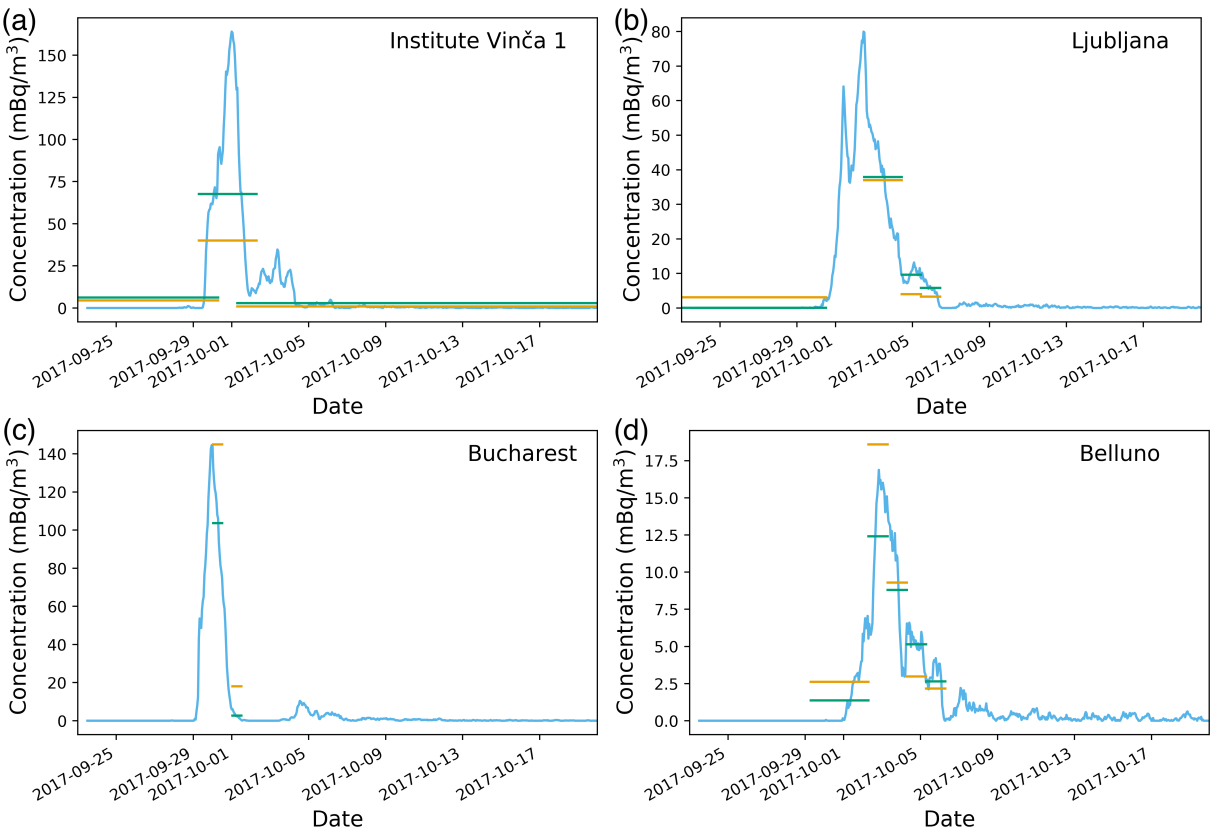

Figure 4: The modelled concentration (blue), measured average concentration (orange) and modelled average concentration (green) of airborne Ruthenium-106 at four measurement sites: (a) Institute Vinča 1 near Belgrade in Serbia, (b) Ljubljana in Slovenia, (c) Bucharest in Romania and (d) Belluno in Italy.

this work. Differences likely arise from the differences in atmospheric transport modelling, the imposed meteorology and the assumption of a finite release made in this work.

An estimate of the release date earlier than that in Masson et al. (2019) is supported by evidence that ^{106}Ru deposits of 50.7 Bq/m^2 per day were measured at Kyshtym, in Russia, between 23 and 24 September 2017 (Roshydromet, 2017). The site of Kyshtym is located in close to the Mayak facility and known to be a contaminated since the 1957 Kyshtym disaster, however total background levels at this site in August 2017 were only 0.7 Bq/m^2 per day (Roshydromet, 2017). Lack of information concerning the timings of this deposition sampling unfortunately limits better knowledge of plausible release times.

The estimated total release of 441 TBq ^{106}Ru is much smaller than the previous release from the Mayak facility during the 1957 Kyshsym disaster, where some 2,700 TBq ^{106}Ru (and its daughter product ^{106}Rh) was released (Jones, 2008). The release of ^{106}Ru is, however, still substantial and considerably greater than other Russian incidents, such as the 1993 accident at the Tomsk-7 reprocessing plant where the ^{106}Ru release was estimated to be only 7.9-11.1 TBq, and 25.3-36.7 TBq for the total activity of all materials released (IAEA, 1998). The Tomsk-7 accident was classified as 4 on the International Nuclear Event Scale (INES), i.e. an accident with local consequences.

The method proposed in this work imposes a finite set of release times. This may not be valid for larger sustained releases but has merits as a method for fast response while maintaining a formal probabilistic framework. The presented method can be extended to a time series estimate by extending the Gibbs step in the algorithm as e.g. Tichý et al. (2017). This would add greater computational expense per grid cell but may be feasible if massively parallel computing facilities are available. The inclusion of temporal correlation, as Tichý et al. (2017), may remove spurious release times, although the effect of smoothing short-term releases should be questioned. Atmospheric releases over a short time period would also be impacted by an imposed release duration. The error in estimation will be greatest when the meteorological temporal variability during and following the release is greatest. It is possible to reduce the release period if necessary, although the temporal resolution of the driving meteorology may limit the resolving power during estimation.

The uncertainty in the current estimated release of ^{106}Ru, is likely to be a lower estimate of uncertainty due the need to impose an idealised statistical model on a physical system. The estimated magnitude of the 2017 release nevertheless demonstrates that the radioactive cloud across Europe was caused by a substantial release.

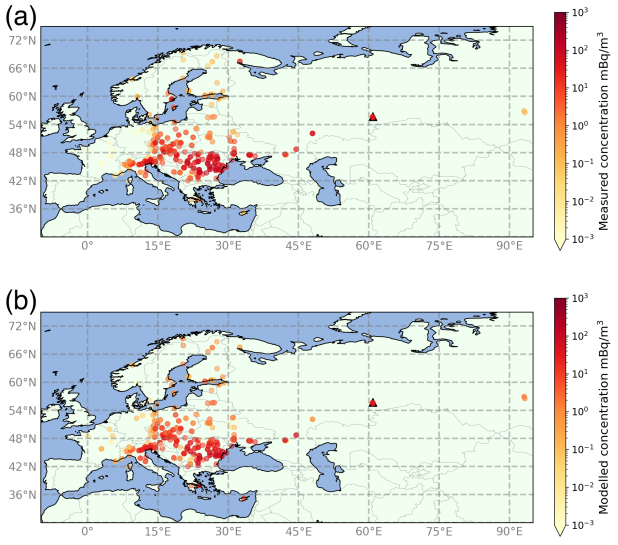

Figure 5: The (a) measured and (b) modelled concentrations of ^{106}Ru at the various measurement sites assuming a release from the Mayak Nuclear Facility between 12:00-18:00 UTC 24 September 2017. The modelled concentrations use the mean posterior estimated release of 441 TBq. The black triangle shows the location of the Mayak nuclear facility.

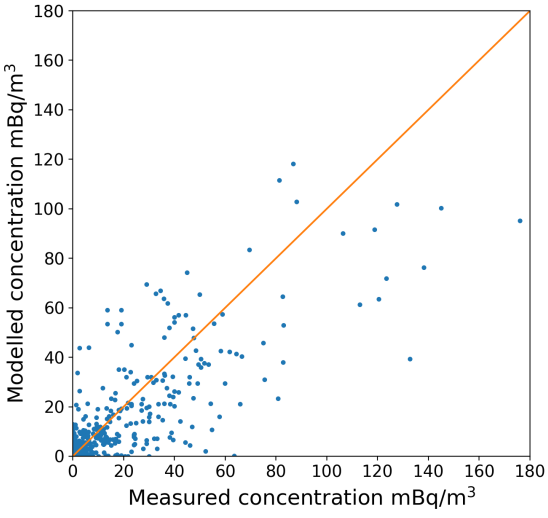

Figure 6: A scatter plot of the measured and modelled concentrations of ^{106}Ru for all measurements assuming a release from the Mayak Nuclear Facility between 12:00-18:00 UTC 24 September 2017. The modelled concentrations use the mean posterior estimated release of 441 TBq.

4. Conclusions

We estimate that the 2017 release of ruthenium-106 most likely originated from the southern Ural region of Russia, supporting other evidence that it may have been caused by a release from the Mayak nuclear facility. This release most likely occurred between 12:00-18:00 UTC 24 September 2017, where a total of 441 TBq ^{106}Ru was release.

This paper presents a novel approach to estimating source properties of a radiological release of a single species with an unknown source location. This method explicitly considers multiple sources of uncertainty by including the site measurement error and using an MCMC approach to estimating the size of the release and simulated transport error. We use Expectation-Maximisation to efficiently estimate the source release time.

The method is aimed at operational implementation, where the sensitivities for each measurement, derived using a Lagrangian transport model, and hierarchical inference can be run in parallel to speed up the overall implementation time. The assumption of a constant release in a single release window decreases the parameter size of the problem, improving the computational tractability and reducing the risk of overfitting, but at the expense of gaining information about temporal variation. Larger, sustained releases from known sources would likely benefit from other approaches within the literature.

The conclusions from this paper only supports suggestions that the release was involved with the production of a large ^{144}Ce source for a neutrino experiment insofar as confirming the likely release location is the Mayak nuclear complex. The size of the release, as suggested by our model, is substantial, even if the threat posed no risk to the wider public.

A. Appendix

This section outlines the algorithm to infer the source emission magnitude, x, the standard deviation of the simulated transport error τ and optimal release time $\hat{t}$ in a set of possible release times $t \in \mathscr{T}$. We inform this using n independent measurements of atmospheric concentration in the vector $\mathbf{y}$, where each measurement has an associated measurement error σ_i whose square forms the diagonal covariance matrix $\mathbf{\Sigma}$, and there is a known mapping between x and $\mathbf{y}$ which is linear for each t, $\mathbf{h}(t)$.

We estimate these parameters using a standard hierarchical Bayesian approach,

$$\mathrm{p}(x, \tau, \hat{t} \mid \mathbf{y}) \propto \mathrm{p}(\mathbf{y} \mid x, \tau, \hat{t})\, \mathrm{p}(x \mid \tau, \hat{t})\, \mathrm{p}(\tau \mid \hat{t})\, \mathrm{p}(\hat{t}). \tag{2}$$

We assign the Jeffreys prior for a Normal distribution for x, meaning that it is non-informative (see e.g. Robert et al., 2009). The transport error is given a uniform prior probability between lower and upper bounds $a = 5$ and $b = 50$ mBq m^{-3} respectively. The time period $t \in \mathscr{T}$ is estimated using an empirical Bayes approach, which does not require any prior information.

Algorithm 1 uses a Gibbs sampler for x, Slice sampler for τ and an Expectation-Maximisation step for t. In the following algorithm $\mathbf{I}$ is the identity matrix, $\mathcal{U}(0,1)$ signifies sampling uniformly between 0 and 1, w is the width parameter for Slice sampling (see Neal, 2003) and $\tilde{\mathrm{p}}(\cdot)$ is the unnormalised log-posterior probability. For sampling τ the unnormalised log-posterior probability is calculated as,

$$\tilde{\mathrm{p}}(x, \tau, \hat{t} \mid \mathbf{y}) = \begin{cases} -\frac{1}{2}\mathrm{tr}\left(\log(\mathbf{\Sigma} + \mathbf{I}\tau^2)\right) - \frac{1}{2}(\mathbf{h}(\hat{t})x - \mathbf{y})^T(\mathbf{\Sigma} + \mathbf{I}\tau^2)^{-1}(\mathbf{h}(\hat{t})x - \mathbf{y}) - \log(b-a) & \text{if } a \le \tau \le b, \\ -\infty & \text{otherwise,} \end{cases} \tag{3}$$

where $\mathrm{tr}(\cdot)$ is the trace of the matrix. The output is the mean and standard deviation of the sampled values of x, disregarding the first 10% as a burn in period, the optimal value for t using the mean sampled value of τ, and the marginal likelihood using these values.

Algorithm 1 Gibbs-Slice-EM algorithm

a = 5
b = 50
w = 2
for t in $\mathscr{T}$ **do**
  $x^*(t) = (\mathbf{h}(t)^T\mathbf{h}(t))^{-1}\mathbf{h}(t)\mathbf{y}$
end for
$\hat{t} = \arg\min_{t \in \mathscr{T}} \sum_j (h(t)_j x^*(t) - y_j)^2$
$x^{(0)} = (\mathbf{h}(\hat{t})^T\mathbf{h}(\hat{t}))^{-1}\mathbf{h}(\hat{t})^T\mathbf{y}$
$\tau^{(0)} = \mathcal{U}(0,1)(b-a)$
for $k = 1$ **to** iterations **do**
  $x^{(k)} \sim \mathcal{N}\left(\left(\mathbf{h}(\hat{t})^T(\mathbf{\Sigma} + \mathbf{I}\tau^{2\,(k-1)})^{-1}\mathbf{h}(\hat{t})\right)^{-1}\mathbf{h}(\hat{t})^T(\mathbf{\Sigma} + \mathbf{I}\tau^{2\,(k-1)})^{-1}\mathbf{y}, \mathbf{h}(\hat{t})^T(\mathbf{\Sigma} + \mathbf{I}\tau^{2\,(k-1)})\mathbf{h}(\hat{t})\right)$ {Gibbs step}
  $u \sim \log(\mathcal{U}(0,1)) + \tilde{\mathrm{p}}(\tau^{(k-1)})$ {Begin Slice step}
  $u' \sim \mathcal{U}(0,1)$
  $\tau_{\min} = \tau^{(k-1)} - u'w$
  $\tau_{\max} = \tau_{\min} + w$
  while $u < \tilde{\mathrm{p}}(\tau_{\min})$ **do**
    $\tau_{\min} = \tau_{\min} - w$
  end while
  while $u < \tilde{\mathrm{p}}(\tau_{\max})$ **do**
    $\tau_{\max} = \tau_{\max} + w$
  end while
  $u'' \sim \mathcal{U}(0,1)$
  $\tau^{(k)} = \tau_{\min} + u''(\tau_{\max} - \tau_{\min})$ {End Slice step}
  $\hat{t} = \arg\min_{t \in \mathscr{T}} \left((\mathbf{h}(t)x^{(k)} - \mathbf{y})^T(\mathbf{\Sigma} + \mathbf{I}\tau^{2\,(k)})^{-1}(\mathbf{h}(t)x^{(k)} - \mathbf{y})\right)$ {Expectation-Maximisation step}
end for

References

Annunzio, A.J., Young, G.S., Haupt, S.E., 2012. Utilizing state estimation to determine the source location for a contaminant. Atmospheric Environment 46, 580–589. URL: http://www.sciencedirect.com/science/article/pii/S1352231011004699, doi:10.1016/j.atmosenv.2011.04.080.

Brunner, D., Henne, S., Keller, C.A., Reimann, S., Vollmer, M.K., O'Doherty, S., Maione, M., 2012. An extended Kalman-filter for regional scale inverse emission estimation. Atmospheric Chemistry and Physics 12, 3455–3478. URL: http://www.atmos-chem-phys.net/12/3455/2012/, doi:10.5194/acp-12-3455-2012.

Cartlidge, E., 2018. Isotope cloud linked to failed neutrino source. Science 359, 729–729. URL: https://science.sciencemag.org/content/359/6377/729, doi:10.1126/science.359.6377.729.

Cervone, G., Franzese, P., 2010. Monte Carlo source detection of atmospheric emissions and error functions analysis. Computers & Geosciences 36, 902–909. URL: http://www.sciencedirect.com/science/article/pii/S0098300410001263, doi:10.1016/j.cageo.2010.01.007.

Delle Monache, L., Lundquist, J.K., Kosović, B., Johannesson, G., Dyer, K.M., Aines, R.D., Chow, F.K., Belles, R.D., Hanley, W.G., Larsen, S.C., Loosmore, G.A., Nitao, J.J., Sugiyama, G.A., Vogt, P.J., 2008. Bayesian Inference and Markov Chain Monte Carlo Sampling to Reconstruct a Contaminant Source on a Continental Scale. Journal of Applied Meteorology and Climatology 47, 2600–2613. URL: http://journals.ametsoc.org/doi/abs/10.1175/2008JAMC1766.1, doi:10.1175/2008JAMC1766.1.

Dempster, A.P., Laird, N.M., Rubin, D.B., 1977. Maximum Likelihood from Incomplete Data via the EM Algorithm. Journal of the Royal Statistical Society. Series B (Methodological) 39, 1–38. URL: https://www.jstor.org/stable/2984875.

Elder, J.C., Graf, J.M., Dewart, J.M., Buhl, T.E., Wenzel, W.J., Walker, L.J., Stoker, A.K., 1986. Guide to radiological accident considerations for siting and design of DOE nonreactor nuclear facilities.

Ganesan, A.L., Rigby, M., Zammit-Mangion, A., Manning, A.J., Prinn, R.G., Fraser, P.J., Harth, C.M., Kim, K.R., Krummel, P.B., Li, S., Mühle, J., O'Doherty, S.J., Park, S., Salameh, P.K., Steele, L.P., Weiss, R.F., 2014. Characterization of uncertainties in atmospheric trace gas inversions using hierarchical Bayesian methods. Atmospheric Chemistry and Physics 14, 3855–3864. URL: http://www.atmos-chem-phys.net/14/3855/2014/, doi:10.5194/acp-14-3855-2014.

Geman, S., Geman, D., 1984. Stochastic Relaxation, Gibbs Distributions, and the Bayesian Restoration of Images. IEEE Transactions on Pattern Analysis and Machine Intelligence PAMI-6, 721–741. doi:10.1109/TPAMI.1984.4767596.

IAEA, 1998. The radiological accident in the reprocessing plant at Tomsk. International Atomic Energy Agency, Vienna.

Jakab, D., Endrődi, G., Kocsonya, A., Pántya, A., Pázmándi, T., Zagyvai, P., 2018. Methods, results and dose consequences of 106ru detection in the environment in Budapest, Hungary. Journal of Environmental Radioactivity 192, 543–550. URL: http://www.sciencedirect.com/science/article/pii/S0265931X18303333, doi:10.1016/j.jenvrad.2018.08.004.

Jones, A., Thomson, D., Hort, M., Devenish, B., 2007. The U.K. Met Office's Next-Generation Atmospheric Dispersion Model, NAME III, in: Air Pollution Modeling and Its Application XVII. Springer US, Boston, MA, pp. 580–589. URL: http://link.springer.com/10.1007/978-0-387-68854-1_62, doi:10.1007/978-0-387-68854-1_62.

Jones, S., 2008. Windscale and Kyshtym: a double anniversary. Journal of Environmental Radioactivity 99, 1–6. URL: http://www.sciencedirect.com/science/article/pii/S0265931X07002512, doi:10.1016/j.jenvrad.2007.10.002.

Liu, Y., Haussaire, J.M., Bocquet, M., Roustan, Y., Saunier, O., Mathieu, A., 2017. Uncertainty quantification of pollutant source retrieval: comparison of Bayesian methods with application to the Chernobyl and Fukushima Daiichi accidental releases of radionuclides. Quarterly Journal of the Royal Meteorological Society 143, 2886–2901. URL: https://rmets.onlinelibrary.wiley.com/doi/abs/10.1002/qj.3138, doi:10.1002/qj.3138.

Lucas, D.D., Simpson, M., Cameron-Smith, P., Baskett, R.L., 2017. Bayesian inverse modeling of the atmospheric transport and emissions of a controlled tracer release from a nuclear power plant. Atmospheric Chemistry and Physics 17, 13521–13543. URL: https://www.atmos-chem-phys.net/17/13521/2017/, doi:10.5194/acp-17-13521-2017.

Maffezzoli, N., Baccolo, G., Di Stefano, E., Clemenza, M., 2019. The Ruthenium-106 plume over Europe in 2017: a source-receptor model to estimate the source region. Atmospheric Environment 212, 239–249. URL: http://www.sciencedirect.com/science/article/pii/S1352231019303322, doi:10.1016/j.atmosenv.2019.05.033.

Manning, A.J., O'Doherty, S., Jones, A.R., Simmonds, P.G., Derwent, R.G., 2011. Estimating UK methane and nitrous oxide emissions from 1990 to 2007 using an inversion modeling approach. Journal of Geophysical Research 116. URL: http://doi.wiley.com/10.1029/2010JD014763, doi:10.1029/2010JD014763.

Masson, O., Steinhauser, G., Wershofen, H., Mietelski, J.W., Fischer, H.W., Pourcelot, L., Saunier, O., Bieringer, J., Steinkopff, T., Hýža, M., Møller, B., Bowyer, T.W., Dalaka, E., Dalheimer, A., de Vismes-Ott, A., Eleftheriadis, K., Forte, M., Gasco Leonarte, C., Gorzkiewicz, K., Homoki, Z., Isajenko, K., Karhunen, T., Katzlberger, C., Kierepko, R., Kövendiné Kónyi, J., Malá, H., Nikolic, J., Povinec, P.P., Rajacic, M., Ringer, W., Rulík, P., Rusconi, R., Sáfrány, G., Sykora, I., Todorović, D., Tschiersch, J., Ungar, K., Zorko, B., 2018. Potential Source Apportionment and Meteorological Conditions Involved in Airborne 131i Detections in January/February 2017 in Europe. Environmental Science & Technology 52, 8488–8500. URL: https://doi.org/10.1021/acs.est.8b01810, doi:10.1021/acs.est.8b01810.

Masson, O., Steinhauser, G., Zok, D., Saunier, O., Angelov, H., Babić, D., Bečková, V., Bieringer, J., Bruggeman, M., Burbidge, C.I., Conil, S., Dalheimer, A., Geer, L.E.D., Ott, A.d.V., Eleftheriadis, K., Estier, S., Fischer, H., Garavaglia, M.G., Leonarte, C.G., Gorzkiewicz, K., Hainz, D., Hoffman, I., Hýža, M., Isajenko, K., Karhunen, T., Kastlander, J., Katzlberger, C., Kierepko, R., Knetsch, G.J., Kónyi, J.K., Lecomte, M., Mietelski, J.W., Min, P., Møller, B., Nielsen, S.P., Nikolic, J., Nikolovska, L., Penev, I., Petrinec, B., Povinec, P.P., Querfeld, R., Raimondi, O., Ransby, D., Ringer, W., Romanenko, O., Rusconi, R., Saey, P.R.J., Samsonov, V., Šilobritienė, B., Simion, E., Söderström, C., Šoštarić, M., Steinkopff, T., Steinmann, P., Sýkora, I., Tabachnyi, L., Todorovic, D., Tomankiewicz, E., Tschiersch, J., Tsibranski, R., Tzortzis, M., Ungar, K., Vidic, A., Weller, A., Wershofen, H., Zagyvai, P., Zalewska, T., García, D.Z., Zorko, B., 2019. Airborne concentrations and chemical considerations of radioactive ruthenium from an undeclared major nuclear release in 2017. Proceedings of the National Academy of Sciences , 16750–16759URL: https://www.pnas.org/content/early/2019/07/25/1907571116, doi:10.1073/pnas.1907571116.

Michalak, A.M., Hirsch, A., Bruhwiler, L., Gurney, K.R., Peters, W., Tans, P.P., 2005. Maximum likelihood estimation of covariance parameters for Bayesian atmospheric trace gas surface flux inversions. Journal of Geophysical Research: Atmospheres 110. URL: https://agupubs.onlinelibrary.wiley.com/doi/abs/10.1029/2005JD005970, doi:10.1029/2005JD005970.

Mietelski, J.W., Povinec, P.P., 2020. Environmental radioactivity aspects of recent nuclear accidents associated with undeclared nuclear activities and suggestion for new monitoring strategies. Journal of Environmental Radioactivity 214-215, 106151. URL: https://linkinghub.elsevier.com/retrieve/pii/S0265931X19308549, doi:10.1016/j.jenvrad.2019.106151.

Neal, R.M., 2003. Slice sampling. The Annals of Statistics 31, 705–767. URL: https://projecteuclid.org/euclid.aos/1056562461, doi:10.1214/aos/1056562461.

Penev, I., Angelov, H., Arsov, T., Georgiev, S., Uzunov, N., 2018. 106Ru Aerosol Activity Observation above Southeast Europe in October 2017. Technical Report. "Prof. Marin Drinov" Publishing House of Bulgarian Academy of Sciences. URL: http://www.proceedings.bas.bg/DOI/doi2018_5_04.html, doi:10.7546/CRABS.2018.05.04.

Ramebäck, H., Söderström, C., Granström, M., Jonsson, S., Kastlander, J., Nylén, T., Ågren, G., 2018. Measurements of 106ru in Sweden during the autumn 2017: Gamma-ray spectrometric measurements of air filters, precipitation and soil samples, and in situ gamma-ray spectrometry measurement. Applied Radiation and Isotopes 140, 179–184. URL: http://

www.sciencedirect.com/science/article/pii/S0969804318301714, doi:10.1016/j.apradiso.2018.07.008.

Robert, C.P., Chopin, N., Rousseau, J., 2009. Harold Jeffreys's Theory of Probability Revisited. Statistical Science 24, 141–172. URL: https://projecteuclid.org/euclid.ss/1263478373, doi:10.1214/09-STS284. publisher: Institute of Mathematical Statistics.

Roshydromet, 2017. Report on the causes and source of ruthenium-106 on the territory of Russia in September-October 2017 [in Russian]. URL: http://egasmro.ru/files/documents/reports/report_28_12_2017.pdf.

Saunier, O., Didier, D., Mathieu, A., Masson, O., Dumont Le Brazidec, J., 2019. Atmospheric modeling and source reconstruction of radioactive ruthenium from an undeclared major release in 2017. Proceedings of the National Academy of Sciences 116, 24991–25000. URL: http://www.pnas.org/lookup/doi/10.1073/pnas.1907823116, doi:10.1073/pnas.1907823116.

Saunier, O., Mathieu, A., Didier, D., Tombette, M., Quélo, D., Winiarek, V., Bocquet, M., 2013. An inverse modeling method to assess the source term of the Fukushima Nuclear Power Plant accident using gamma dose rate observations. Atmospheric Chemistry and Physics 13, 11403–11421. URL: https://www.atmos-chem-phys.net/13/11403/2013/, doi:10.5194/acp-13-11403-2013.

Shershakov, V.M., Borodin, R.V., Tsaturov, Y.S., 2019. Assessment of Possible Location Ru-106 Source in Russia in September–October 2017. Russian Meteorology and Hydrology 44, 196–202. URL: https://doi.org/10.3103/S1068373919030051, doi:10.3103/S1068373919030051.

Stohl, A., Seibert, P., Wotawa, G., Arnold, D., Burkhart, J.F., Eckhardt, S., Tapia, C., Vargas, A., Yasunari, T.J., 2012. Xenon-133 and caesium-137 releases into the atmosphere from the Fukushima Dai-ichi nuclear power plant: determination of the source term, atmospheric dispersion, and deposition. Atmospheric Chemistry and Physics 12, 2313–2343. URL: https://www.atmos-chem-phys.net/12/2313/2012/acp-12-2313-2012.html, doi:https://doi.org/10.5194/acp-12-2313-2012.

Sørensen, J.H., 2018. Method for source localization proposed and applied to the October 2017 case of atmospheric dispersion of Ru-106. Journal of Environmental Radioactivity 189, 221–226. URL: http://www.sciencedirect.com/science/article/pii/S0265931X18300146, doi:10.1016/j.jenvrad.2018.03.010.

Tichý, O., Šmídl, V., Hofman, R., Šindelářová, K., Hýža, M., Stohl, A., 2017. Bayesian inverse modeling and source location of an unintended ^{131}I release in Europe in the fall of 2011. Atmospheric Chemistry and Physics 17, 12677–12696. URL: https://www.atmos-chem-phys.net/17/12677/2017/, doi:10.5194/acp-17-12677-2017.

Walters, D.N., Williams, K.D., Boutle, I.A., Bushell, A.C., Edwards, J.M., Field, P.R., Lock, A.P., Morcrette, C.J., Stratton, R.A., Wilkinson, J.M., Willett, M.R., Bellouin, N., Bodas-Salcedo, A., Brooks, M.E., Copsey, D., Earnshaw, P.D., Hardiman, S.C., Harris, C.M., Levine, R.C., MacLachlan, C., Manners, J.C., Martin, G.M., Milton, S.F., Palmer, M.D., Roberts, M.J., Rodríguez, J.M., Tennant, W.J., Vidale, P.L., 2014. The Met Office Unified Model Global Atmosphere 4.0 and JULES Global Land 4.0 configurations. Geoscientific Model Development 7, 361–386. URL: https://www.geosci-model-dev.net/7/361/2014/, doi:10.5194/gmd-7-361-2014.

Western, L.M., Sha, Z., Rigby, M., Ganesan, A.L., Manning, A.J., Stanley, K.M., O'Doherty, S.J., Young, D., Rougier, J., 2020. Bayesian spatio-temporal inference of trace gas emissions using an integrated nested Laplacian approximation and Gaussian Markov random fields. Geoscientific Model Development 13, 2095–2107. URL: https://www.geosci-model-dev.net/13/2095/2020/, doi:10.5194/gmd-13-2095-2020.

Yee, E., Lien, F.S., Keats, A., D'Amours, R., 2008. Bayesian inversion of concentration data: Source reconstruction in the adjoint representation of atmospheric diffusion. Journal of Wind Engineering and Industrial Aerodynamics 96, 1805–1816. URL: http://www.sciencedirect.com/science/article/pii/S0167610508000482, doi:10.1016/j.jweia.2008.02.024.